Journal of Computational Physics **174,** 852–869 (2001)
doi:10.1006/jcph.2001.6941, available online at http://www.idealibrary.com on IDEAL®

Logarithmic Singularities in Two-Body, Bound-State Integral Equations

G. B. Mainland

Department of Physics, The Ohio State University at Newark, Newark, Ohio 43055
E-mail: mainland@mps.ohio-state.edu

Received March 7, 2001; revised August 23, 2001

A logarithmic singularity is typically present in the kernels of two-body, bound-state integral equations after the two angular variables associated with three-dimensional spherical coordinates are separated. The singularity occurs in the separated Schrödinger equation, the separated Bethe–Salpeter equation in the instantaneous approximation, and the partially separated Bethe–Salpeter equation. Problems integrating over the singularity have restricted the types of basis functions that have been used to obtain numerical solutions, making it particularly difficult to obtain bound-state solutions that decrease rapidly at both small and large momenta. Here integrals are evaluated analytically in the neighborhood of the singularity by expanding the integrands, excluding the singular kernels, either analytically or numerically in a Taylor series or a Maclaurin series. This technique makes possible the use of nonpolynomial basis functions that satisfy the boundary conditions, allowing the efficient calculation of all solutions.

Key Words: bound-state integral equation; Bethe–Salpeter equation; instantaneous approximation; logarithmic singularity.

1. INTRODUCTION

The Bethe–Salpeter equation [1], which is based on field theory, is covariant, and reduces to the Schrödinger equation in the nonrelativistic limit, is an appropriate equation to use in describing relativistic bound states. Typically the Bethe–Salpeter equation is an integral equation although, at least in some cases, it can be expressed as a differential equation. If a two-body, bound-state Bethe–Salpeter equation is rotationally invariant in three-dimensional space, the two angular variables associated with three-dimensional spherical coordinates can be separated. When written in integral form, after the two angular variables are separated a logarithmic singularity is present in the kernels. While this singularity is not the primary reason that the Bethe–Salpeter equation is often so difficult to solve [2], the singularity complicates obtaining solutions.

0021-9991/01 $35.00

Since, even numerically, the two-body, bound-state Bethe–Salpeter equation often cannot readily be solved, various approximations such as the Blankenbecler–Sugar approximation [3] or the instantaneous approximation [1, 4] are often made that reduce the covariant equation in four dimensions to an approximately covariant integral equation in three dimensions. The instantaneous approximation, which is the approximation that the binding quanta travel instantaneously between the bound constituents, was first introduced in the original article by Bethe and Salpeter [1] and was used to demonstrate that the Schrödinger equation is the nonrelativistic limit of the Bethe–Salpeter equation. More in the spirit of this work, Salpeter [4] made the instantaneous approximation to reduce the Bethe–Salpeter equation to a three-dimensional equation and calculated corrections to the fine structure of hydrogen-like atoms. A major difficulty in solving equations numerically when the instantaneous approximation is made arises because a logarithmic singularity occurs in the kernel of the integral equations after the angular dependence of solutions is separated.

Gammel and Menzel [5] deal with the logarithmic singularity by using a special weighting scheme in the neighborhood of the singularity. Kwon and Tabakin [6] and Di Leo and Darewych [6] use a subtraction technique that isolates the singularity in an integral that can be evaluated analytically. Silvestre-Brac, *et al.* [7] use splines (see, for example, [8]) as basis functions and then use recursion relations so that the various integrals are written in terms of a single integral that is calculated analytically. Eyre and Vary [9] introduce a numerical cutoff and then correct for the effects of the cutoff using perturbation theory. Later Spence and Vary [10] used splines [8] as basis functions and evaluate all integrals analytically. Since splines are polynomials, their method and that of Ref. [7] are restricted to polynomial basis functions. In this article methods are used to integrate analytically over the logarithmic singularity that allow the use of nonpolynomial basis functions that satisfy the boundary conditions. Specifically, in an ϵ-neighborhood of the singularity, excluding the Legendre functions of the second kind that contain the singularity, integrands are expanded either analytically or numerically in either a Taylor series or a Maclaurin series, making it possible to evaluate the integrals analytically in the ϵ-neighborhood. For bound-state solutions that decrease rapidly at small and large momenta, which for the Schrödinger equation are typically solutions with larger angular momentum, if solutions can be obtained at all, significantly more basis functions must be used when the solution is expanded in terms of basis functions that do not satisfy the boundary conditions.

To estimate the accuracy of each solution, the left- and right-hand sides of the equation are calculated at a series of points, and a reliability coefficient [11], which is a statistical measure of how accurately the left- and right-hand sides agree at the selected points, is calculated. Examining points where the left- and right-hand sides of the equation agree least well reveals possible problems with trial solutions and suggests possible remedies.

The effectiveness of the methods for integrating over the singularity is demonstrated by using basis functions that satisfy the boundary conditions to obtain numerical, bound-state solutions for a spin-0 and spin-$1/2$ constituent that interact via minimal electrodynamics, both in the nonrelativistic limit and in the instantaneous approximation. Bound states of a spin-0 and spin-$1/2$ constituent are of interest because they have been proposed as composite models of leptons, either when the two particles interact electromagnetically [12] or when they interact through a stronger force [13]. However, the methods demonstrated here for integrating over logarithmic singularities apply equally well to the more commonly studied bound state of two spin-$1/2$ particles. The presence of a derivative coupling in the interaction complicates the construction of the Bethe–Salpeter equation in the

instantaneous approximation and yields an equation that contains both a single integral and a double integral with singular kernels.

2. DERIVATION AND SEPARATION OF THE BETHE–SALPETER EQUATION IN THE INSTANTANEOUS APPROXIMATION

When a spin-0 field $\phi(x)$, which represents a quanta with charge Q and mass M, interacts via minimal electrodynamics with a spin-1/2 field $\Psi(x)$, which represents a quanta with charge q and mass m, the renormalizable Lagrangian is [14]

$$\begin{aligned} L =: & [(i\partial^\mu - QA^\mu)\phi^\dagger][(-i\partial_\mu - QA_\mu)\phi] - M^2\phi^\dagger\phi \\ & + \bar{\Psi}\gamma_\mu(i\partial^\mu - qA^\mu)\Psi - m\bar{\Psi}\Psi - \frac{1}{4}F_{\mu\nu}F^{\mu\nu} :, \end{aligned} \tag{2.1}$$

where $F_{\mu\nu} = \partial_\nu A_\mu - \partial_\mu A_\nu$.

Following standard procedures [1], in the ladder approximation the Bethe–Salpeter equation describing a bound state of a spin-0 boson and a spin-1/2 fermion is

$$\begin{aligned} & (p^\mu\gamma_\mu + \xi K^\mu\gamma_\mu - m)\{[p^\mu - (1-\xi)K^\mu][p_\mu - (1-\xi)K_\mu] - M^2\}\chi_K(p) \\ & \quad = \frac{iqQ}{(2\pi)^4}\int_{-\infty}^{\infty}\frac{d^4q}{(p-q)^2 + i\epsilon}[p^\mu\gamma_\mu + q^\mu\gamma_\mu - 2(1-\xi)K^\mu\gamma_\mu]\chi_K(q). \end{aligned} \tag{2.2}$$

In (2.2), K^μ is the four-momentum of the bound state, and ξ is the parameter that appears in the definition of center-of-mass coordinates. Nonrelativistically $\xi = m/(m+M)$, but when the instantaneous approximation is made, ξ cancels out of the Bethe–Salpeter equation.

The instantaneous approximation [1, 4] is made by making the replacement

$$\frac{1}{(p-q)^2 + i\epsilon} = \frac{1}{(p_0 - q_0)^2 - (\mathbf{p}-\mathbf{q})^2 + i\epsilon} \to \frac{1}{-(\mathbf{p}-\mathbf{q})^2 + i\epsilon} \tag{2.3}$$

in the photon propagator in (2.2). Defining

$$\Psi_K(\mathbf{q}) \equiv \int_{-\infty}^{\infty} dq_0\, \chi_K(q) \quad \text{and} \quad \phi_K(\mathbf{q}) \equiv \int_{-\infty}^{\infty} dq_0\, q_0\, \chi_K(q), \tag{2.4}$$

the integral over q_0 in (2.2) can be carried out immediately. Going to the center-of-momentum frame where $K^\mu = (E, 0)$, (2.2) becomes

$$\begin{aligned} & [p^0\gamma^0 - p^i\gamma^i + \xi E\gamma_0 - m]\{[p^0 - (1-\xi)E]^2 - p^i p^i - M^2\}\chi_E(p) \\ & \quad = -\frac{iqQ}{(2\pi)^4}\int_{-\infty}^{\infty}\frac{d^3q}{(\mathbf{p}-\mathbf{q})^2}[\gamma^0 p^0 - \gamma^i(p^i + q^i) - 2(1-\xi)E\gamma^0]\Psi_E(\mathbf{q}) \\ & \qquad - \frac{iqQ}{(2\pi)^4}\int_{-\infty}^{\infty}\frac{d^3q}{(\mathbf{p}-\mathbf{q})^2}\gamma^0\phi_E(\mathbf{q}), \end{aligned} \tag{2.5}$$

where $\chi_E(p)$ is the value of $\chi_K(p)$ in the center-of-momentum frame.

Solving (2.5) for $\chi_E(p)$, integrating over p^0 on both sides of the equation, and using (2.4) yield

$$\omega_M(p)E\Psi_E(\mathbf{p}) = \frac{\omega_M(p)}{\omega_m(p)}[\omega_M(p)+\omega_m(p)][\gamma^0\gamma^i p^i + \gamma^0 m]\Psi_E(\mathbf{p}) + \frac{qQ}{16\pi^3}\int_{-\infty}^{\infty}\frac{d^3q}{(\mathbf{p}-\mathbf{q})^2}\left\{(1-\xi)E + \left[\frac{\omega_M(p)+\omega_m(p)}{\omega_m(p)}\right]\gamma^0\gamma^i p^i + \frac{\omega_M(p)}{\omega_m(p)}\gamma^0 m + \gamma^0\gamma^i q^i\right\}\Psi_E(\mathbf{q}) - \frac{Qq}{16\pi^3}\int_{-\infty}^{\infty}\frac{d^3q}{(\mathbf{p}-\mathbf{q})^2}\phi_E(\mathbf{q}), \quad (2.6)$$

where $\omega_M(p) \equiv (M^2 + \mathbf{p}\cdot\mathbf{p})^{1/2}$, etc. Equation (2.6) cannot readily be solved because of the presence of the two functions Ψ_E and ϕ_E that are related as indicated in (2.4). The function ϕ_E is present, of course, as a consequence of the derivative coupling. It is possible, however, to express ϕ_E in terms of Ψ_E as follows: By dividing both sides of (2.5) by $\{[p^0-(1-\xi)E]^2 - p^i p^i - M^2\}$ and then integrating over p^0, a second equation that involves both Ψ_E and ϕ_E is obtained. Subtracting the second equation from (2.6) and solving for $\phi_E(\mathbf{p})$ yield

$$\phi_E(\mathbf{p}) = (1-\xi)E\Psi_E(\mathbf{p}) - \frac{1}{\omega_m(p)}(\gamma^0\gamma^i p^i + \gamma^0 m) \times \left[\omega_M(p)\Psi_E(\mathbf{p}) + \frac{qQ}{16\pi^3}\int_{-\infty}^{\infty}\frac{d^3q}{(\mathbf{p}-\mathbf{q})^2}\Psi_E(\mathbf{q})\right]. \quad (2.7)$$

Using (2.7) to express $\phi_E(\mathbf{p})$ in terms of Ψ_E, (2.6) becomes the Bethe–Salpeter equation in the instantaneous approximation:

$$\omega_M(p)E\Psi_E(\mathbf{p}) = \frac{\omega_M(p)}{\omega_m(p)}[\omega_M(p)+\omega_m(p)][\gamma^0\gamma^i p^i + \gamma^0 m]E\Psi_E(\mathbf{p}) + \frac{qQ}{16\pi^3}\int_{-\infty}^{\infty}\frac{d^3q}{(\mathbf{p}-\mathbf{q})^2}\left\{\left[\frac{\omega_M(p)}{\omega_m(p)}+1\right]\gamma^0\gamma^i p^i + \left[\frac{\omega_M(q)}{\omega_m(q)}+1\right]\gamma^0\gamma^i q^i + \left[\frac{\omega_M(p)}{\omega_m(p)} + \frac{\omega_M(q)}{\omega_m(q)}\right]\gamma^0 m\right\}\Psi_E(\mathbf{q}) + \frac{(qQ)^2}{4(2\pi)^6}\int_{-\infty}^{\infty}\frac{d^3q}{(\mathbf{p}-\mathbf{q})^2} \times \frac{m\gamma^0 + \gamma^0\gamma^i q^i}{\omega_m(q)}\int_{-\infty}^{\infty}\frac{d^3k}{(\mathbf{q}-\mathbf{k})^2}\Psi_E(\mathbf{k}). \quad (2.8)$$

For consistency, if the term proportional to $(qQ)^2$ in the above equation is retained, the crossed and "seagull" diagrams, which also contribute terms proportional to $(qQ)^2$, should be included in constructing the Bethe–Salpeter equation. Here the term is retained to illustrate the somewhat different numerical techniques that are required to evaluate double integrals, each of which has a kernel with a logarithmic singularity.

Equation (2.8) is much easier to solve numerically than the Bethe–Salpeter equation, primarily because it is much easier to obtain solutions with real energy eigenvalues. Specifically, equations of the form (2.8) can be solved numerically by converting them to matrix eigenvalue equations. When each side is multiplied by $\Psi_E^\dagger(\mathbf{p})$ and integrated over d^3p, excluding the eigenvalue E, the quantity on the left-hand side is Hermitian and positive definite and the quantity on the right-hand side is Hermitian. As a consequence the energy eigenvalues must be real (see, for example, [15]). In the very special cases where the

Bethe–Salpeter equation possess the Hermiticity properties of (2.8), the equation is relatively easy to solve numerically [2, 16] in spite of the fact that after separation of the two angular variables, it is still an integral or partial differential equation in two variables.

Solutions to (2.8) are of the form

$$\Psi_E(\mathbf{p}) = \begin{bmatrix} G^{(\pm)}(p)\phi^{(\pm)}(\theta,\varphi) \\ F^{(\pm)}(p)\phi^{(\mp)}(\theta,\varphi) \end{bmatrix}, \tag{2.9}$$

where the $\phi^{(\pm)}(\theta,\varphi)$ are the same functions [14] that represent the angular dependence of the bound-state solutions to the Dirac equation when the potential is spherically symmetric. After the angular integration is performed using Hecke's theorem [17, 18, 12], the angular variables separate. The separated equation is written in terms of dimensionless variables by rewriting the masses as $m \equiv m_0(1-\Delta)$ and $M \equiv m_0(1+\Delta)$. The dimensionless momentum p' is defined by $p' \equiv p/m_0$ and the dimensionless energy ε by

$$\varepsilon \equiv \frac{E}{M+m} = \frac{E}{2m_0}. \tag{2.10}$$

Multiplying the resulting upper and lower equations by p' and $-p'$, respectively, and omitting primes since all variables are now dimensionless, in the instantaneous approximation the separated Bethe–Salpeter equation is

$$\begin{aligned}
&2\varepsilon\omega_+(p)\begin{bmatrix} pG^{(\pm)}(p) \\ pF^{(\pm)}(p) \end{bmatrix} \\
&\quad = \frac{\omega_+(p)}{\omega_-(p)}[\omega_+(p)+\omega_-(p)]\left\{ p\begin{bmatrix} pF^{(\pm)}(p) \\ pG^{(\pm)}(p) \end{bmatrix} + (1-\Delta)\begin{bmatrix} pG^{(\pm)}(p) \\ -pF^{(\pm)}(p) \end{bmatrix}\right\} \\
&\qquad + \frac{qQ}{8\pi^2}p\left[\frac{\omega_+(p)}{\omega_-(p)}+1\right]\int dq \begin{bmatrix} qF^{(\pm)}(q)Q_{j\pm\frac{1}{2}}\left(\frac{p^2+q^2}{2pq}\right) \\ qG^{(\pm)}(q)Q_{j\mp\frac{1}{2}}\left(\frac{p^2+q^2}{2pq}\right) \end{bmatrix} \\
&\qquad + \frac{qQ}{8\pi^2}\int q\,dq\left[\frac{\omega_+(q)}{\omega_-(q)}+1\right]\begin{bmatrix} qF^{(\pm)}(q)Q_{j\mp\frac{1}{2}}\left(\frac{p^2+q^2}{2pq}\right) \\ qG^{(\pm)}(q)Q_{j\pm\frac{1}{2}}\left(\frac{p^2+q^2}{2pq}\right) \end{bmatrix} \\
&\qquad + \frac{qQ}{8\pi^2}(1-\Delta)\int dq\left[\frac{\omega_+(p)}{\omega_-(p)}+\frac{\omega_+(q)}{\omega_-(q)}\right]\begin{bmatrix} qG^{(\pm)}(q)Q_{j\mp\frac{1}{2}}\left(\frac{p^2+q^2}{2pq}\right) \\ -qF^{(\pm)}(q)Q_{j\pm\frac{1}{2}}\left(\frac{p^2+q^2}{2pq}\right) \end{bmatrix} \\
&\qquad + \frac{(qQ)^2}{4(2\pi)^4}\int\frac{dq}{\omega_-(q)}\int dk\left\{(1-\Delta)\begin{bmatrix} kG^{(\pm)}(k)Q_{j\mp\frac{1}{2}}\left(\frac{k^2+q^2}{2kq}\right)Q_{j\mp\frac{1}{2}}\left(\frac{p^2+q^2}{2pq}\right) \\ -kF^{(\pm)}(k)Q_{j\pm\frac{1}{2}}\left(\frac{k^2+q^2}{2kq}\right)Q_{j\pm\frac{1}{2}}\left(\frac{p^2+q^2}{2pq}\right) \end{bmatrix}\right. \\
&\qquad \left. + q\begin{bmatrix} kF^{(\pm)}(k)Q_{j\pm\frac{1}{2}}\left(\frac{k^2+q^2}{2kq}\right)Q_{j\mp\frac{1}{2}}\left(\frac{p^2+q^2}{2pq}\right) \\ kG^{(\pm)}(k)Q_{j\mp\frac{1}{2}}\left(\frac{k^2+q^2}{2kq}\right)Q_{j\pm\frac{1}{2}}\left(\frac{p^2+q^2}{2pq}\right) \end{bmatrix}\right\},
\end{aligned} \tag{2.11}$$

where $Q_{j\pm1/2}$ is a Legendre function of the second kind and $\omega_\pm(p) \equiv [(1\pm\Delta)^2+p^2]^{1/2}$.

The set of two equations with the top signs is transformed into the set of two equations with the bottom signs and vice versa with the following replacements:

$$G^{(+)} \leftrightarrow F^{(-)}, \quad F^{(+)} \leftrightarrow -G^{(-)}, \quad \varepsilon \leftrightarrow -\varepsilon. \tag{2.12}$$

As a consequence only the equations for $F^{(+)}$ and $G^{(+)}$ need be solved. For notational convenience the superscripts on $F^{(+)}$ and $G^{(+)}$ are omitted in future equations.

3. SOLUTIONS TO THE NONRELATIVISTIC REDUCTION OF THE BETHE–SALPETER EQUATION

In this section the nonrelativistic reduction of the Bethe–Salpeter equation, which is just the Schrödinger equation, is solved numerically in momentum space. Although the equation can be solved analytically [18], here it is solved numerically to illustrate one technique that will be used to solve the Bethe–Salpeter equation in the instantaneous approximation, an equation that, apparently, cannot in general be solved analytically. A method is introduced for handling the singularity in the kernel that makes possible the use of basis functions that satisfy the boundary conditions both at small and large momenta. For angular momentum states $\ell = 0$ and $\ell = 1$, these basis functions are not as improvement over the basis functions used in Refs. [7] and [10] that only automatically satisfy the boundary conditions for small momenta, but for angular momentum states $\ell > 1$, the basis functions used here converge to a solution much more efficiently.

Once the instantaneous approximation has been made, it is straightforward to make a nonrelativistic reduction [1]. Keeping the lowest order term in the interaction,

$$E'\Psi(\mathbf{p}) = \left(\frac{\mathbf{p}^2}{2M} + \frac{\mathbf{p}^2}{2m}\right)\Psi(\mathbf{p}) + \frac{qQ}{8\pi^3}\int_{-\infty}^{\infty} \frac{d^3q}{(\mathbf{p}-\mathbf{q})^2}\Psi(\mathbf{q}). \tag{3.1}$$

The nonrelativistic energy E' is related to the relativistic energy E by $E = m + M + E'$.

To solve (3.1) a dimensionless momentum $\mathbf{p}'$ is defined by

$$\mathbf{p}' \equiv \frac{\mathbf{p}}{\sqrt{-2\mu E'}}, \tag{3.2}$$

where μ is the reduced mass. Equation (3.1) then becomes

$$(1 + \mathbf{p}'^2)\Psi(\mathbf{p}') = \frac{qQ}{4\pi}\frac{\sqrt{-2\mu E'}}{2\pi^2 E'}\int_{-\infty}^{\infty} \frac{d^3q'}{(\mathbf{p}'-\mathbf{q}')^2}\Psi(\mathbf{q}'). \tag{3.3}$$

Equation (3.3) is the integral form of the Schrödinger equation for a quanta with mass μ and charge q interacting with a stationary charge Q via the Coulomb potential. Since the momentum variables are all now dimensionless, for notational convenience the primes will be omitted.

The solution is of the form

$$\Psi(\mathbf{p}) = R(p)Y_\ell^m(\theta, \phi). \tag{3.4}$$

Using Hecke's theorem [17, 18, 12] the angular integration is easily performed. The angular dependence separates, yielding the integral equation

$$(1+p^2)pR(p) = \lambda\frac{2}{\pi}\int_0^\infty dq\; Q_\ell\left(\frac{p^2+q^2}{2pq}\right) qR(q), \tag{3.5}$$

where

$$\lambda \equiv \frac{qQ}{4\pi}\sqrt{\frac{-\mu}{2E'}} = \ell + n, \quad n = 1,\, 2, \ldots . \tag{3.6}$$

Equation (3.5) would be straightforward to solve numerically were it not for the fact that the Legendre function of the second kind, $Q_\ell((p^2+q^2)/2pq)$, has a logarithmic singularity at $p = q$.

The boundary conditions are determined with the aid of the asymptotic relationship [19]

$$Q_\ell(z) \underset{z\to\infty}{\longrightarrow} \frac{\sqrt{\pi}\Gamma(\ell+1)}{2^{\ell+1}\Gamma\left(\ell+\frac{3}{2}\right)}\frac{1}{z^{\ell+1}}. \tag{3.7}$$

At small p the function $pR(p)$ has the form

$$pR(p) \underset{p\to 0}{\longrightarrow} p^{c_0}, \tag{3.8}$$

where c_0 is a constant. From (3.7) it follows that at small p, $Q_\ell((p^2+q^2)/2pq) \to p^{\ell+1}$. Equating the left- and right-hand sides of (3.5), at small p the equality $pR(p) \sim p^{\ell+1}$ is obtained, implying

$$c_0 = \ell + 1. \tag{3.9}$$

Using analogous logic, at large p the function $pR(p)$ has the form

$$pR(p) \underset{p\to\infty}{\longrightarrow} \frac{1}{p^{\ell+3}}. \tag{3.10}$$

Solutions are obtained by expanding $pR(p)$ in terms of N cubic splines $B_j(p)$ [8],

$$pR(p) = F(p)\sum_{j=1}^{N} c_j B_j(p). \tag{3.11}$$

By choosing the convergence function $F(p)$ in (3.11) so that at small and large p it behaves as the solution $pR(p)$ itself, fewer splines are required to accurately represent solutions that go to zero rapidly at the boundaries.

Cubic splines are defined on five consecutive knots. To determine the spacing of the knots, $N-4$ zeros x_i of a Chebychev polynomial are calculated using the formula

$$x_i = -\cos\frac{(2i-1)\pi}{2(N-4)}, \quad i = 1,\, 2, \ldots,\, N-4, \tag{3.12}$$

and then the knots T_{i+4} on the positive p axis are determined by

$$T_{i+4} = C_1\sqrt{\frac{1+x_i}{1-x_i}} + C_2, \quad i = 1,\ 2,\ \ldots,\ N-4, \tag{3.13}$$

where C_1 and C_2 are constants. The knot T_4 is placed at the origin and three knots are placed on the "negative" p axis to create maximum freedom in constructing the solution $pR(p)$ near the origin. The three knots on the "negative" p axis are mirror images of the first three knots in (3.13).

Spence and Vary [10] note that integrals of the form

$$\int_0^\infty dp\ p^{\ell+k} Q_\ell\left(\frac{p^2+q^2}{2pq}\right), \quad k = 0,\ 1,\ 2,\ \ldots \tag{3.14}$$

are both finite and readily calculated analytically, so they choose $F(p)$ in (3.11) so that the boundary conditions are satisfied near $p = 0$ provided that the sum of splines in (3.11) is nonzero and slowly changing near the origin. That is, $F(p) = p^{\ell+1}$. Since the splines vanish at the largest knot, an appropriate sum of splines will satisfy the boundary condition at large p. However, the boundary conditions are satisfied both at small and at large p with the choice

$$F(p) = \frac{p^{\ell+1}}{(c^2+p^2)^{\ell+\frac{3}{2}}}, \tag{3.15}$$

where c is a constant. Note that at small p, $F(p) \to p^{\ell+1}$ as expected from (3.9), while at large p, $F(p) \to p^{-(\ell+2)}$, which is one power of p less than is indicated in (3.10). Since the last spline in the expansion (3.11) vanishes at the largest knot, the boundary conditions will be satisfied for both small and large momenta provided that the sum of splines in (3.11) is slowly changing at small momenta and goes to zero as the reciprocal of the momentum at large momenta. By choosing $F(p)$ in (3.11) to be given by (3.15), accurate solutions that decrease rapidly at small and large momenta can be obtained.

Equation (3.5) is solved numerically by converting the integral eigenvalue equation into a generalized matrix equation using the Rayleigh–Ritz–Galerkin method [20]. The solution is expanded in terms of splines using (3.11), and then both sides of (3.5) are multiplied by $B_i(p)F(p)$ and integrated over p. A generalized matrix equation results that is of the form $Ac = \lambda Bc$, where the matrices A and B are given, respectively, by

$$A_{ij} = \int_0^\infty dp B_i(p)F(p)(1+p^2)F(p)B_j(p) \tag{3.16a}$$

and

$$B_{ij} = \frac{2}{\pi}\int_0^\infty dp B_i(p)F(p)\int_0^\infty dq\, Q_\ell\left(\frac{p^2+q^2}{2pq}\right)F(q)B_j(q). \tag{3.16b}$$

The elements of the column vector c are the expansion coefficients c_j in (3.11). Since both of the above matrices are symmetric and A is positive definite, the eigenvalues are real [15].

The choice $F(p) = p^{\ell+1}$ works well for small values of angular momentum because the sum of a small number of splines readily creates a function that decreases as $p^{-(2\ell+4)}$ at large p, thus satisfying the boundary condition as given in (3.10). In addition, when $F(p) = p^{\ell+1}$, the integrals over $Q_\ell((p^2+q^2)/2pq)$ in (3.16b) can be performed analytically because they are of the form (3.14). For larger values of angular momentum, however, the choice $F(p) = p^{\ell+1}$ does not work well because the sum of a small number of splines does not readily create a function that decreases sufficiently rapidly at large momentum to satisfy the boundary conditions.

The choice (3.15) for the convergence function immediately allows the boundary conditions to be satisfied by a sum of splines that is slowly changing, but now the integrals over q in (3.16b) can no longer be readily performed analytically. Integration over the singular kernel is accomplished as follows: Except in an ϵ-neighborhood of the singularity, all integrations are performed numerically using Gaussian quadrature with a seven-point option. As the integration variable approaches the singularity, where the kernel changes most rapidly, integration intervals are decreased to maintain accuracy of the numerical integration. Within an ϵ-neighborhood of the singularity, the integrand, excluding the singular Legendre function of the second kind, $Q_\ell((p^2+q^2)/2pq)$, is expanded in a Taylor series about the singularity. In the ϵ-neighborhood of the singularity the integral is then a sum of integrals of the form (3.14) that can be integrated analytically. The parameter ϵ is chosen to be the smaller of 0.01 or the distance from the singularity to the nearest knot, thus avoiding the complication of integrating over a knot.

To obtain a numerical estimate of the accuracy of each solution, the left- and right-hand sides of (3.5) are calculated midway between each pair of knots on the (positive) p axis. A reliability coefficient r, which is a statistical measure of how closely the two sides of the equation agree at selected points, is calculated using the formula [11]

$$r \equiv 1 - \frac{\frac{1}{N_{pts}} \Sigma_{i=1}^{N_{pts}} (LHS_i - RHS_i)^2}{\frac{1}{N_{pts}-1} \left\{ \Sigma_{i=1}^{N_{pts}} (LHS_i + RHS_i)^2 - \frac{1}{N_{pts}} \left[\Sigma_{i=1}^{N_{pts}} (LHS_i + RHS_i) \right]^2 \right\}}, \tag{3.17}$$

where LHS_i and RHS_i are, respectively, the values of the left- and right-hand sides of the equation at the ith point. If the two sides of the equation agree exactly at all of the selected points, then r equals unity. Determining where the left- and right-hand sides of the equation agree least well reveals possible problems with trial solutions.

When $F(p) = p^{\ell+1}$, excellent solutions are obtained for $\ell = 0$ and $\ell = 1$: With 21 splines in the expansion (3.11), eigenvalues are correct to four or five significant figures and corresponding r-values are in the range $0.999 < r < 1.00$. However, when $\ell = 2$, as shown in the second and third columns of Table I, an incorrect eigenvalue appears with a corresponding $r = 0.00112$. For $\ell = 3$, the first few eigenvalues are accurate, but the corresponding r-values have magnitudes on the order of or less than 10^{-3}, indicating that the solutions are unsatisfactory. Examination of these solutions reveals that the left- and right-hand sides of the equation do not agree near the the boundaries. By choosing the convergence factor $F(p)$ as given in (3.15), the difficulties that appeared for $\ell > 1$ are eliminated, as can be seen from the fourth and fifth columns of Table I.

The advantage of using basis functions that obey the boundary conditions is further illustrated in Fig. 1. The exact radial wave function in momentum space [18] is graphed for the state 7F, which is the state corresponding to the final entry in Table I. Numerical

TABLE I
Numerical Values of $\lambda = \ell + 1, \ell + 2, \ldots$ When 21 Splines Are Used in the Expansion (3.11)

	$F(p) = p^{\ell+1}$		$F(p) = p^{\ell+1}/(c^2 + p^2)^{\ell+3/2}$	
ℓ	λ	r	λ	r
2	3.00000	0.99884	3.00000	1.0000
	4.00007	0.97013	4.00001	1.0000
	4.49547	0.00112	5.00003	1.0000
	5.00030	0.84320	6.00008	1.0000
3	4.00118	0.00266	4.00000	1.0000
	5.00844	−0.00028	5.00000	1.0000
	6.02762	−0.00031	6.00004	1.0000
	7.06566	−0.00023	6.99999	1.0000

solutions for the radial wave function are also graphed when the convergence functions $F(p) = p^{\ell+1}/(c^2 + p^2)^{\ell+3/2}$ and $F(p) = p^{\ell+1}$ are used. The radial wave function calculated with the convergence function $F(p) = p^{\ell+1}/(c^2 + p^2)^{\ell+3/2}$, which provides basis functions that obey the boundary conditions, is so close to the exact solution that the two curves cannot be distinguished on the graph. However, for the solution calculated with $F(p) = p^{\ell+1}$, the left- and right-hand sides of the equation do not agree at small and large momentum p because the basis functions do not satisfy the boundary condition at large momentum.

4. SOLUTIONS IN THE INSTANTANEOUS APPROXIMATION

Solutions to the Bethe–Salpeter equation in the instantaneous approximation are obtained using two different basis systems. The first basis system comprises essentially the same basis functions that were employed to calculate solutions in the nonrelativistic case. Because the basis functions vanish at large momenta, they are particularly suitable for representing solutions that have significant support only to moderately large values of momentum (and position). For this basis system, four splines are nonzero between consecutive knots in the

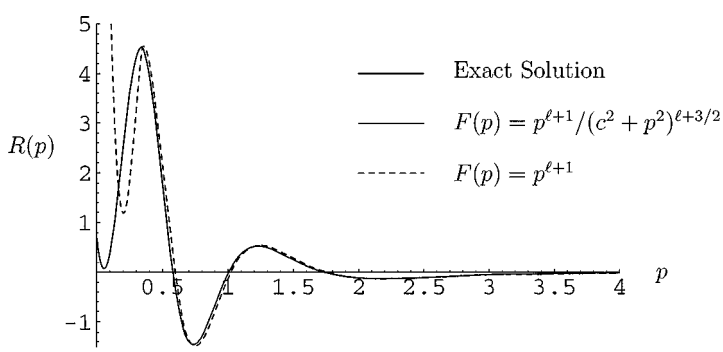

FIG. 1. The radial hydrogen wave function for the state 7F in momentum space as a function of the dimensionless momentum p.

physical region except for the final four knots at the largest values of momentum: There the number of nonzero splines between consecutive knots decreases from three to two until only one spline is nonzero between the final two knots, thus making it increasingly difficult to represent solutions at large momenta. To better represent solutions that are highly localized in position space and, therefore, have significant support at large values of momentum, a second basis system is used in which some basis functions vanish only at infinite values of momentum, and four splines are nonzero between all knots in the physical region.

The boundary conditions as p approaches zero and infinity are determined using the same procedure employed in the previous section. The results are as follows:

$$pG(p) \underset{p\to 0}{\longrightarrow} p^{j+\frac{1}{2}}, \quad pF(p) \underset{p\to 0}{\longrightarrow} p^{j+\frac{3}{2}}, \tag{4.1a}$$

$$pG(p) \underset{p\to \infty}{\longrightarrow} \frac{1}{p^{j+\frac{3}{2}}}, \quad pF(p) \underset{p\to \infty}{\longrightarrow} \frac{1}{p^{j+\frac{5}{2}}}. \tag{4.1b}$$

Solutions can be obtained using methods of the previous section and are of the form

$$pG(p) = \mathcal{G}_1(p) \sum_{j=1}^{N} g_j B_j(p), \quad pF(p) = \mathcal{F}_1(p) \sum_{j=1}^{N} f_j B_j(p). \tag{4.2}$$

The convergence functions $\mathcal{G}_1(p)$ and $\mathcal{F}_1(p)$ are chosen so that the boundary conditions are automatically satisfied provided that the sums of splines in the previous equation are slowly changing for small and large momenta:

$$\mathcal{G}_1(p) = \frac{p^{j+\frac{1}{2}}}{(c_{\mathcal{G}}^2 + p^2)^{j+\frac{1}{2}}}, \quad \mathcal{F}_1(p) = \frac{p^{j+\frac{3}{2}}}{(c_{\mathcal{F}}^2 + p^2)^{j+\frac{3}{2}}}. \tag{4.3}$$

In the above equation $c_{\mathcal{G}}$ and $c_{\mathcal{F}}$ are constants. At small p, $p\mathcal{G}_1(p)$ and $p\mathcal{F}_1(p)$ vanish as indicated in (4.1a), but at large p they decrease by a factor p more slowly than indicated in (4.1b) because the splines themselves vanish at large p. As can be seen from (4.3), solutions go to zero rapidly at the boundaries even at the smallest value $j = 1/2$, so it would be difficult to obtain solutions in the instantaneous approximation without using convergence functions that obey the boundary conditions at both small and large momenta.

Equation (2.11) is converted into a generalized matrix equation of the form

$$A \begin{bmatrix} g \\ f \end{bmatrix} = \varepsilon B \begin{bmatrix} g \\ f \end{bmatrix} \tag{4.4}$$

by multiplying the top and bottom equations by $\mathcal{G}_1(p)B_i(p)$ and $\mathcal{F}_1(p)B_i(p)$, respectively, and then integrating over p. The elements of the column vectors g and f are, respectively, the expansion coefficients g_j and f_j in (4.2). Since the matrices A and B have been constructed so that both are symmetric and B is positive definite, the dimensionless energy eigenvalue ε is forced to be real [15] as required.

The Bethe–Salpeter equation in the instantaneous approximation contains double integrals, while in the nonrelativistic limit the equation involves only single integrals. In spite of this complication, by performing integrations in a specific order, all integrals with a logarithmic singularity that are necessary to solve the equation are of the form already

encountered in the previous section. However, the technique used to integrate over the logarithmic singularity in the previous section fails at very large values of momentum: All of the terms being expanded in a Taylor series about the singular point p are functions of q^2 with the result that a typical term in the expansion is $a_n(q^2 - p^2)^n$. Within an ϵ-neighborhood of p, the maximum value of $q^2 - p^2$ is of the order $2p\epsilon$. When p is on the order of $1/\epsilon$, the expansion loses accuracy. By choosing ϵ to decrease linearly with increasing p, this problem is avoided.

To check the accuracy of the solutions by calculating the reliability coefficient, double integrals of the following form must be evaluated:

$$\int_0^\infty \frac{dq}{\omega_-(q)} Q_\ell\left(\frac{p^2+q^2}{2pq}\right) \int_0^\infty dk\, Q_\ell\left(\frac{k^2+q^2}{2kq}\right) \frac{q^{\ell+d_1}}{(c^2+k^2)^{d_2}} B_j(k). \tag{4.5}$$

The integral over the variable k can be calculated as previously discussed. Except within an ϵ-neighborhood of the logarithmic singularity of the integrand, the integral over the variable q is evaluated numerically. Within the ϵ-neighborhood, the integral over k is expressed as a Taylor series in the variable q,

$$\int_0^\infty dk\, Q_\ell\left(\frac{k^2+q^2}{2kq}\right) \frac{q^{\ell+d_1}}{(c^2+k^2)^{d_2}} B_j(k) = q^{\ell+1} \sum_{j=0}^{3} a_j (q-p)^j. \tag{4.6}$$

The Taylor series in the previous equation depends on the fact that the integral vanishes as $q^{\ell+1}$ at small q, a fact that is readily verified using (3.7). The coefficients a_j are determined numerically so that the expansion and the integral agree at $q = p + \epsilon$, $p + \epsilon/3$, $p - \epsilon/3$, and $p - \epsilon$. Using the expansion in (4.6), within the ϵ-neighborhood of the logarithmic singularity at p, the integral (4.5) can be performed analytically.

To better represent solutions that are highly localized in position space and, therefore, have significant support at large values of momentum, a second basis system is introduced in which some basis functions vanish only at infinity. To construct the basis system, the momentum is first mapped onto a compact space with the transformation

$$x(p^2) = b\frac{p^2 - a}{p^2 + a}, \tag{4.7}$$

where a and b are constants.

The knots are determined by first calculating $N - 8$ zeros x_i of a Chebychev polynomial using the formula

$$x_i = -\cos\frac{(2i-1)\pi}{2(N-8)}, \quad i = 1, 2, \ldots, N-8. \tag{4.8}$$

The knots in the region $-b < x < b$ are then given by

$$T_{i+4} = bx_i, \quad i = 1, 2, \ldots, N-8. \tag{4.9}$$

The knot T_4 is placed at $x = -b$ ($p = 0$), and three knots are placed in the region $x < -b$ (on the "negative" p axis) to create maximum freedom in constructing solutions near the origin. The three knots in the region $x < -b$ are mirror images of the first three knots in

(4.9). In a similar fashion the knot T_{N-3} is placed at $x = b$ ($p = \infty$), and three knots are placed in the region $x > b$ ($p > \infty$). With the above knot structure, four splines are nonzero between each pair of adjacent knots in the physical region.

The solution is expanded in terms of splines,

$$pG(p) = \mathcal{G}_2(p(x)) \sum_{j=1}^{N} g_j B_j(x), \quad pF(p) = \mathcal{F}_2(p(x)) \sum_{j=1}^{N} f_j B_j(x), \tag{4.10}$$

where

$$\mathcal{G}_2(p) = \frac{p^{j+\frac{1}{2}}}{\left(c_{\mathcal{G}}^2 + p^2\right)^{j+1}}, \quad \mathcal{F}_2(p) = \frac{p^{j+\frac{3}{2}}}{\left(c_{\mathcal{F}}^2 + p^2\right)^{j+2}}. \tag{4.11}$$

For the second basis system the final three splines in the expansion are nonzero at $x = b$ ($p = \infty$). Consequently, solutions that have significant support at large values of momentum are more readily expressed in terms of the second set of basis functions. Since some splines are finite at $p = \infty$, the functions $\mathcal{G}_2(p)$ and $\mathcal{F}_2(p)$ are chosen to satisfy the boundary conditions (4.1) both at small and at large momenta.

To integrate over singularities at large values of momentum q, it is easier to evaluate the integral if the integrand is expanded in a Maclaurin series in the variable $1/q$ instead of in a Taylor series in q because the Maclaurin series converges efficiently from the knot to infinity. Specifically, if the location of the first knot less than the singularity corresponds to a value of momentum equal to or less than 50, then integrals are evaluated as previously discussed. However, if the first knot less than the singularity corresponds to a value of momentum greater than 50, the integral is evaluated numerically from $x = -b$ ($p = 0$) to the knot. From the knot to $x = b$ ($p = \infty$), the integral is evaluated analytically by expanding the integrand, excluding the Legendre function of the second kind, in a Maclaurin series. While the transition value of momentum (50) is somewhat arbitrary, the value must be sufficiently large that the MacLaurin series converges efficiently with just four terms. The necessary formulas for carrying out the integration are given in the Appendix.

A corresponding modification is required to evaluate the double integrals (4.5). When the location of the first knot less than the logarithmic singularity at $q = p$ corresponds to a value of p equal to or less than 50, the integral is evaluated as before. When the position of the knot corresponds to a value of p greater than 50, the integral is evaluated numerically except within an ϵ-neighborhood of the singularity. Within the ϵ-neighborhood, the integrals over k are expanded as a Maclaurin series,

$$\int_0^\infty dk\, Q_\ell\left(\frac{k^2+q^2}{2kq}\right) \frac{q^{\ell+d_1}}{(c^2+k^2)^{d_2}} B_j(k) = \frac{1}{q^{\ell+1}} \sum_{j=0}^{3} a_j \frac{1}{q^j}. \tag{4.12}$$

The coefficients a_j are determined numerically so that the expansion and the integral agree at $q = p + \epsilon$, $p + \epsilon/3$, $p - \epsilon/3$, and $p - \epsilon$. Using the expansion in (4.12), within the ϵ-neighborhood of the logarithmic singularity at p, the integral (4.5) can be performed analytically.

The first basis system has more knots concentrated at small values of momentum and, therefore, is more suitable for representing weakly bound solutions or solutions with detailed structure in this region. The second basis system has more knots at large values of momentum

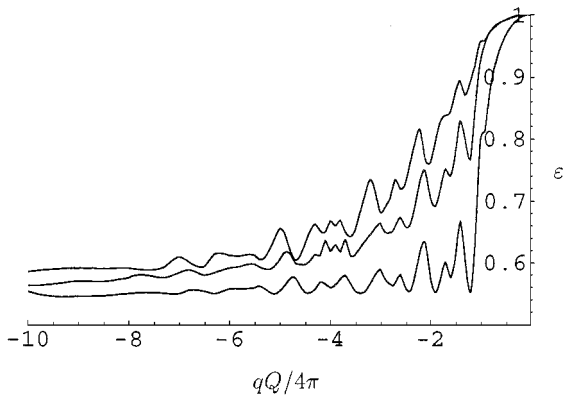

FIG. 2. The dimensionless energy eigenvalues $\varepsilon = E/(M+m)$ of the states $1S_{1/2}$, $2P_{1/2}$, and $2S_{1/2}$ as a function of the coupling constant $qQ/4\pi$ in the instantaneous approximation.

and is better for representing strongly bound solutions that have significant support at large values of momentum. However, at least when 35 or fewer splines are used, the second basis system does not adequately represent the most strongly bound solutions with ε on the order of or less than about 0.3.

For the solutions graphed in Figs. 2 and 3, the constituent masses are equal, although solutions with unequal constituent masses are no more difficult to determine. Solutions are calculated using the two different basis systems previously discussed. For values of $\varepsilon \equiv E/(M+m) > 0.95$, the graphed results are those obtained from the first basis system, which has more knots at small momenta. For all other values of ε, the graphs are an average of the solutions obtained from the two basis systems. Comparing solutions for ε obtained from the two basis systems provides an additional indication of accuracy. The solutions for ε almost always agree to within 0.04 and usually agree more closely, while reliability coefficients are almost always greater than 0.99. Solutions are calculated by expanding the radial wave function in terms of 35 splines.

In comparing Figs. 2 and 3, notice that as the coupling constant decreases in magnitude, the repulsive effects of angular momentum become increasingly apparent so that for states with the same coupling constant, those with higher angular momentum are more weakly bound.

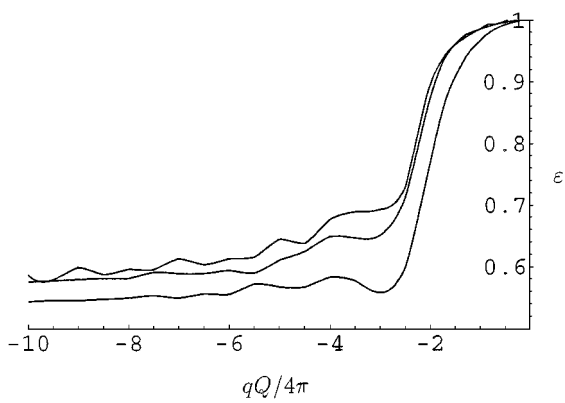

FIG. 3. The dimensionless energy eigenvalues $\varepsilon = E/(M+m)$ of the states $2P_{3/2}$, $3D_{3/2}$, and $3P_{3/2}$ as a function of the coupling constant $qQ/4\pi$ in the instantaneous approximation.

The curves in Figs. 2 and 3 exhibit oscillatory behavior that is different from analytical and numerical solutions of similar equations: For solutions of the one-body Dirac and Klein–Gordon equations with a Coulomb potential, as the absolute value of the coupling constant $|qQ/4\pi|$ increases, the bound-state energy decreases monotonically and, above a critical value of $|qQ/4\pi|$, no real energy eigenvalues exist. Dykshoorn *et al.* [21] found solutions with this same behavior using a variational principle to numerically solve integral equations for bound states in QED within a limited Fock-space approximation. By including the effects of the crossed ladder diagrams, Brezin *et al.* [22] obtained a formula for the bound-state energy of two charged particles that also decreases monotonically as the magnitude of the coupling constant increases.

In the limit that one of the constituent particles becomes infinitely massive, the two-body Bethe–Salpeter equation does not reduce to the corresponding one-body relativistic equation unless the crossed graph is included [23]. As a consequence, the solutions obtained here should not agree with those of the Dirac equation in the limit that M becomes infinite or with the Klein–Gordon equation in the limit that m becomes infinite because the ladder approximation has been made. If the crossed graph were included in the Bethe–Salpeter equation before making the instantaneous approximation, the oscillatory behavior in Figs. 2 and 3 would vanish in the limit that either of the constituent particles became infinitely massive.

5. SUMMARY

A logarithmic singularity is typically present in the kernels of two-body, bound-state integral equations after the two angular variables associated with three-dimensional spherical coordinates are separated. Because of difficulty integrating over this singularity, heretofore numerical solutions have often been calculated using basis functions that do not satisfy the boundary conditions, making it particularly difficult to obtain bound-state solutions that decrease rapidly at both small and large momenta. Here integrals with the singular kernel are evaluated for a wide variety of basis functions: Integrations are performed numerically except within the neighborhood of the singularity where the integration is performed analytically by expanding the integrands, excluding the singular kernels, either analytically or numerically in a Taylor series or a Maclaurin series.

The basis functions used are the product of a "convergence" function and a spline. The convergence function is chosen so that if the sum of the splines is slowly changing, the boundary conditions are automatically satisfied. There are two significant advantages to using basis functions that satisfy the boundary conditions: (i) Fewer basis functions are typically required to obtain accurate solutions. (ii) In cases where the solution decreases rapidly at both small and large momenta, it is exceeding difficult if not almost impossible to obtain numerical solutions unless such basis functions are employed.

Two rather different basis systems are used to calculate solutions. In the first basis system the splines vanish at large momenta, making them particularly suitable for representing weakly bound solutions. The second basis system is more appropriate for calculating strongly bound states because some basis functions vanish only at infinite values of momentum, thereby better representing solutions that are highly localized in position space and, therefore, have significant support at large values of momentum.

To obtain an estimate of the accuracy of each solution, a reliability coefficient is calculated that is a statistical measure of how closely the left- and right-hand sides of the equation agree at a series of selected points.

APPENDIX: CALCULATION OF INTEGRALS

Here formulas are given for calculating the integrals of the form

$$B^{\ell,k}_{(a,b)}(p) \equiv \int_a^b dq\, Q_\ell\left(\frac{p^2+q^2}{2pq}\right)\frac{1}{q^{\ell+k}}, \quad \begin{matrix}\ell = 0, & k = 1,2,3,\ldots,\\ \ell \geq 1, & k = 0,1,2,\ldots\end{matrix} \tag{A1}$$

that are required to integrate over the logarithmic singularities when they occur at large p. Using the recursion formula for Legendre functions of the second kind [24],

$$Q_{\ell+1}(z) = \frac{2\ell+1}{\ell+1} z Q_\ell(z) - \frac{\ell}{\ell+1} Q_{\ell+1}(z), \tag{A2}$$

a recursion relation for $B^{\ell,k}_{(a,b)}(p)$ follows immediately:

$$B^{\ell+1,k}_{(a,b)}(p) = \frac{2\ell+1}{\ell+1}\left[\frac{p}{2} B^{\ell,k+2}_{(a,b)}(p) + \frac{1}{2p} B^{\ell,k}_{(a,b)}(p)\right] - \frac{\ell}{\ell+1} B^{\ell-1,k+2}_{(a,b)}(p). \tag{A3}$$

The integrals $B^{\ell,k}_{(a,b)}(p)$ are readily expressed in terms of the integrals

$$I^k_{(a,b)}(p) \equiv \int_a^b dq \frac{\ln(q+p)}{q^k}. \tag{A4}$$

Specifically,

$$B^{0,k}_{(a,b)}(p) = I^k_{(a,b)}(p) - I^k_{(a,b)}(-p) \tag{A5}$$

and

$$B^{1,k}_{(a,b)}(p) = \frac{p}{2}\left[I^{k+2}_{(a,b)}(p) - I^{k+2}_{(a,b)}(-p)\right] + \frac{1}{2p}\left[I^k_{(a,b)}(p) - I^k_{(a,b)}(-p)\right] + \left\{\begin{matrix} -\ln\left(\frac{b}{a}\right) & \text{if } k = 0 \\ \frac{1}{k}\left[\frac{1}{b^k} - \frac{1}{a^k}\right] & \text{if } k > 0 \end{matrix}\right\}. \tag{A6}$$

The integrals $I^0_{(a,b)}(p)$ and $I^1_{(a,b)}(p)$ are calculated using standard tables of integrals [24], although $I^1_{(a,b)}(p)$ is evaluated as an infinite series. For $k \geq 2$, the integral $I^k_{(a,b)}(p)$ can be calculated using the following formula for the integral I:

$$I \equiv \int dx \frac{\ln(a+bx)}{x^k}, \quad k \geq 2. \tag{A7}$$

Integrating by parts gives

$$I = \frac{1}{k-1}\left[-\frac{\ln(a+bx)}{x^{k-1}} + b\int \frac{dx}{x^{k-1}(a+bx)}\right].$$

The integral in the above expression is evaluated using partial fractions, yielding the desired formula:

$$I = \frac{1}{k-1}\left[-\frac{\ln(a+bx)}{x^{k-1}} + \left(-\frac{b}{a}\right)^{k-1}\ln(a+bx) - \left(-\frac{b}{a}\right)^{k-1}\ln(x) + \sum_{j=2}^{k-1}\left(-\frac{b}{a}\right)^{k-j}\frac{1}{(j-1)x^{j-1}}\right]. \tag{A8}$$

ACKNOWLEDGMENTS

I thank Professor John J. Skowronski for very helpful discussions regarding statistical parameters that would indicate the reliability of numerical solutions to equations. Dr. David G. Robertson assisted in optimizing the code. This work was supported by a grant of computer time from the Ohio Supercomputer Center.

REFERENCES

1. E. E. Salpeter and H. A. Bethe, A relativistic equation for bound-state problems, *Phys. Rev.* **84**, 1232 (1951).
2. G. B. Mainland, Numerical method for solving two-body, bound-state Bethe–Salpeter equations for unequal constituent masses, *Few Body Syst.* **26**, 27 (1999).
3. R. Blankenbecler and R. Sugar, Linear integral equations for relativistic multichannel scattering, *Phys. Rev.* **142**, 1051 (1966).
4. E. E. Salpeter, Mass corrections to the fine structure of hydrogen-like atoms, *Phys. Rev.* **87**, 328 (1952).
5. J. L. Gammel and M. T. Menzel, Beth–Salpeter equation: Numerical experience with a hydrogenlike atom, *Phys. Rev.* **A7**, 858 (1973).
6. Y. R. Kwon and F. Tabakin, Hadronic atoms in momentum space, *Phys. Rev.* **C18**, 932 (1978); L. Di Leo and J. W. Darewych, Bound and resonant relativistic two-particle states in scalar quantum field theory, *Can. J. Phys.* **70**, 412 (1992).
7. B. Silvestre-Brac, A. Bilal, C. Gignoux, and P. Schuck, On the validity of various approximations for the Bethe–Salpeter equation and their WKB quantization, *Phys. Rev.* **D29**, 2275 (1984).
8. C. de Boor, *A Practical Guide to Splines* (Springer-Verlag, Berlin/Heidelberg/New York, 1978).
9. D. Eyre and J. P. Vary, Solving momentum-space integral equations for quarkonia spectra with confining potentials, *Phys. Rev.* **D34**, 3467 (1986).
10. J. R. Spence and J. P. Vary, Solving momentum-space integral equations for quarkonium spectra with confining potentials. II, *Phys. Rev.* **D35**, 2191 (1987); Solving momentum-space integral equations for quarkonium spectra with confining potentials. III. Bethe–Salpeter equation with spin, *Phys. Rev.* **C47**, 1282 (1993).
11. B. J. Winer, *Statistical Principles in Experimental Design* (McGraw–Hill, New York, 1962).
12. G. B. Mainland, Electromagnetic binding of a minimally interacting, relativistic spin-0 and spin-1/2 constituent: Zero four-momentum solutions, *J. Math. Phys.* **27**, 1344 (1986).
13. M. Bander, T. W. Chiu, G. L. Shaw, and D. Silverman, Deeply bound composite fermion with Dirac magnetic moment, *Phys. Rev. Lett.* **47**, 549 (1981).
14. The notation is that of J. D. Bjorken and S. D. Drell, *Relativistic Quantum Fields* (McGraw–Hill, New York, 1965). The constants $\hbar$ and c are set to unity. Repeated Greek indices are summed from 0 to 3 and repeated Roman indices are summed from 1 to 3. Bold variables represent vectors in three-dimensional space.
15. F. B. Hildebrand, *Methods of Applied Mathematics*, 2nd ed. (Prentice Hall, Englewood Cliffs, NJ, 1965).
16. C. Schwartz, Solution of a Bethe–Salpeter equation, *Phys. Rev.* **137**, B717 (1965); M. J. Zuilhof and J. A. Tjon, Electromagnetic properties of the deuteron and the Bethe–Salpeter equation with one-boson exchange, *Phys. Rev.* **C22**, 2369 (1980); G. B. Mainland and J. R. Spence, Numerical solutions to the partially separated, equal-mass, Wick–Cutkosky model, *Few Body Syst.* **19**, 109 (1995); T. Nieuwenhuis and J. A. Tjon, $O(4)$ expansion of the ladder Bethe–Salpeter equation, *Few Body Syst.* **21**, 167 (1996).

17. E. Hecke, Über orthogonal-invariante integralgleichungen, *Math. Ann.* **78**, 398 (1918).
18. V. Fock, Zur theorie des wasserstoffatoms, *Z. Phys.* **98**, 145 (1935); M. Levy, Wave equations in momentum space, *Proc. R. Soc. London Ser. A* **204**, 145 (1950).
19. P. M. Morse and H. Feshbach, *Methods of Theoretical Physics* (McGraw–Hill, New York, 1953).
20. K. E. Atkinson, *A Survey of Numerical Methods for the Solution of Fredholm Equations of the Second Kind* (Soc. for Industr. & Appl. Math., Philadelphia, 1976); L. M. Delves and J. Walsh, *Numerical Solution of Integral Equations* (Clarendon, Oxford, 1974).
21. W. Dykshoorn, R. Koniuk, and R. Muñoz-Tapia, Parity doubling at the critical point in tightly bound systems, *Phys. Lett. B* **229**, 132 (1989).
22. E. Brezin, C. Itzykson, and J. Zinn-Justin, Relativistic Balmer formula including recoil effects, *Phys. Rev.* **D1**, 2349 (1970).
23. F. Gross, Relativistic few-body problem. I. Two-body equations, *Phys. Rev.* **C26**, 2203 (1982).
24. I. S. Gradshteyn and I. M. Ryzhik, *Tables of Integrals, Series, and Products* (Academic Press, New York, 1965).